Liquid Crystalline Thiadiazole Derivatives: Thiadiazole Derivatives Containing Pyridine Ring as Terminal Group

XU, Yan(徐艳) ZHU, Zhi-Guo(朱志国) XU, Zheng*(徐正)

State Key Laboratory of Coordination Chemistry, Coordination Chemistry Institute, Nanjing University, Nanjing, Jiangsu 210093, China

The synthesis and mesomorphic behavior of a new series of liquid crystals containing 1,3,4-thiadiazole and pyridine rings with -CH=N- central group are reported. All compounds exhibit enantiotropic smectic A mesophase, but the Schiff's base analogues have no mesomorphic behavior. The influence of the pyridine ring and thiadiazole ring is discussed.

Keywords Liquid crystal, thiadiazole, pyridine, properties

A great number of mesomorphic compounds containing heterocyclic units have been synthesized, and interest in such structures constantly grows because of the greater possibilities to obtain new mesogenic molecules.[1,2] The heteroatoms can significantly change the polarity, polarizability and sometimes the geometry of the molecule, thereby can influence the type of mesophase, the phase transition temperatures, dielectric constants and other properties of the mesogens.[3]

Heterocyclic compounds like pyridine and pyrimidine derivatives[4] are valuable liquid-crystalline materials for technical applications. It has also been reported that thiadiazole[5-8] may be incorporated into the molecular structure of calamitic mesogens. Here we report the synthesis and mesomorphic behaviour of a series of new Schiff's bases containing both 1, 3, 4-thiadiazole ring and pyridine ring. In these compounds the pyridine ring can occupy the terminal position. The molecular structure is similar to that of stilbazole.

Recently, a novel family of liquid crystalline compounds is built through intermolecular hydrogen bonding by mixing H-bond donor and acceptor moieties.[9] These compounds often show more stable mesophases than either of the individual components if the structure is designed properly. Those molecules bearing 4′-pyridyl moieties are often used as H-bond acceptor. On the other hand, the pyridinic ligands can also coordinate with metals (Rh, Ir, Pt, Pd, Ag) to form metallomesogens.[10] In order to study the mesomorphic behaviour of those novel liquid crystals, we synthesize compound I (Scheme 1). Unexpectedly, these compounds also exhibit enantiotropic mesophases.

Scheme 1

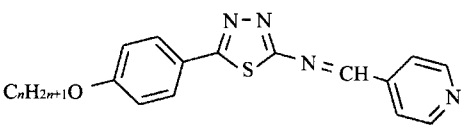

I$_n$, n=4−10

Experimental

The products were synthesized following the reactions shown in Scheme 2.

The compound **2** was prepared from etherification between **1** and BrC_nH_{2n+1} (n = 4—10). The thiosemicarbazone (compound **3**) can be easily obtained by the one-pot condensation procedure. Then the aminothiadiazole (**4**) was prepared via a mild cyclization proceduce. Finallly, the condensation reaction between compound **4**

* Tel: 025-3593133, Fax:025-3314502, E-mail: profzxu@jlonline.com

Received November 7, 2000; revised April 6, 2001; accepted April 30, 2001.

Project supported by the National Natural Science Foundation of China.

and 4-pyridinecarboxaldehyde under the catalysis of piperidine in dried DMF gave the compound $\mathbf{I}_n$.

Scheme 2

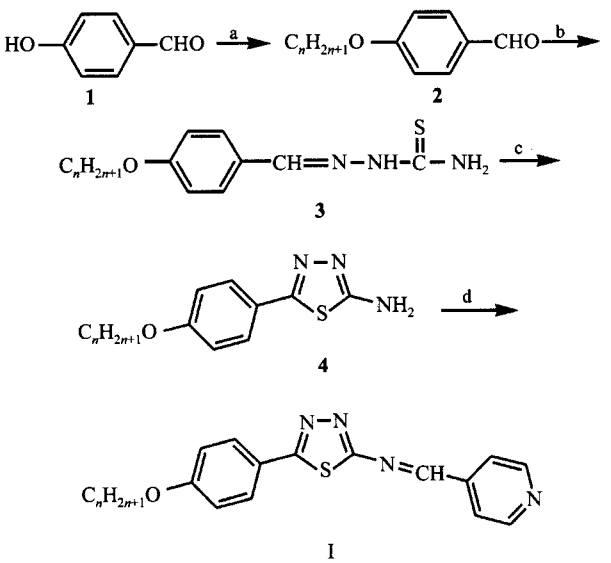

Reagents and condition: a, BrC_nH_{2n+1}, cyclohexanone, K_2CO_3, reflux; b, $NH_2NHCSNH_2$, 95% C_2H_5OH, reflux; c, 1) $FeCl_3 \cdot 6H_2O$, 95% C_2H_5OH, reflux; 2) conc. HCl, $-10°$—0℃; 3) aq. NH_3; d, DMF, 4-pyridinecarboxaldehyde, 120℃.

Infrared (IR) spectra were recorded on an IDP-440 IR spectrometer (KBr plates). Proton nuclear magnetic resonance spectra (^{1}H NMR) were recorded on a Bruker AM500 spectrometer in C_6D_6 solvent. Mass spectrometry (MS) was carried out on a VG-ZAB-HS mass spectrometer (EI). Elemental analysis was completed on a Perkin-Elmer 240C microanalyzer. Differential scanning calorimetry (DSC) was recorded on an ORTHOLUX II Perkin-Elmer DSC-7C at heating rate 10℃ per min. A Leitz polarizing microscope equipped with a hot stage was used to identify the various mesophases. The heating rate was 2℃ per min.

p-Alkoxybenzaldehydes *p*-Hydroxy-benzaldehyde was treated with various alkyl bromides and anhydrous potassium carbonate in cyclohexanone, respectively, by the known method.[11]

4-Alkoxybenzaldehyde-3-thiosemicarbazone Equimolar quantities of *p*-alkoxybenzaldehyde and finely powdered thiosemicarbazide were dissolved in 95% ethanol and refluxed for 30—60 min. The reaction mixture was cooled down to room temperature, and separated by filter to give crystalline 4-alkoxybenzaldehyde-3-thiosemicarbazone (85—90%).

2-Amino-5-(4-alkoxyphenyl)-1, 3, 4-thiadiazole[12]

A mixture of fine powder of thiosemicarbazone (0.01 mol) and ferric chloride hexahydrate (0.04 mol) in 95% ethanol (90 mL) was refluxed gently for 1.5—2 h. Most of the ethanol was removed under reduced pressure, the residue was cooled in an ice-salt bath and then treated with conc. hydrochloric acid (8 mL). The acidic mixture was kept in the ice-salt bath for 2 h, and the precipitated hydrochloride was collected. The free base was liberated after adding some aq. ammonia and heating in a water-bath for 15 min. The aminothiadiazole was extracted from the iron residues with boiling ethanol. Concentrating the ethanolic extract gave the crude amino compound (60%).

Schiff's Base $\mathbf{I}_n$ (n = 4—10) Schiff's Base $\mathbf{I}_n$ (n = 4—10) was prepared by the condensation of equimolar quantities of 2-amino-5-(4-alkoxyphenyl)-1,3, 4-thiadiazole and 4-pyridinecarboxaldehyde in the minimum amount of anhydrous DMF and piperidine (0.20 mL). The reaction mixture was refluxed for 6—10 h. Most of the solvent was removed under reduced pressure, the residue was cooled, then the formed yellow solid was filtered off and recrystallized from anhydrous acetonitrile and dried to give yellow flaky crystals of compound $\mathbf{I}_n$ (n = 4,5,6,7,8,9,10) with yield of 85—90%.

The compounds $\mathbf{I}_{a\text{-}g}$ were characterized by IR, ^{1}H NMR, MS and elemental analysis in excellent agreement with the target compounds. All data are as follows.

$\mathbf{I}_a$ (n = 4) ν_{max}(KBr): 2910 (m, C—H), 1620 (s, N=C), 1610, 1510 (s, Ar), 1250, 1180 (s, C—O) cm^{-1}; δ_H(C_6D_6): 8.73 (s, 1H, -N=CH-), 8.71 (d, J = 10 Hz, 2H, pyridine-H), 8.02 (d, J = 10 Hz, 2H, ArH), 7.25 (d, J = 5 Hz, 2H, pyridine-H), 6.84 (d, J = 5 Hz, 2H, ArH), 3.63—3.59 (m, 2H, CH_2—O), 1.90—0.92 (m, 7H, C_3H_7); m/z (%): 338.2 (M^+,100), 337.2 (M^+-1, 55.7), 281.0 (HOC_6H_4-C_2N_2S-N=C-$C_5H_4N^+$, 73.2), 137.0 (24.8), 57.1 (14.4), 43.0 (23.5). Anal. $C_{18}H_{18}N_4OS$. Calcd: C, 63.91; H, 5.33; N, 16.57. Found: C, 63.28; H, 5.83; N, 16.84.

$\mathbf{I}_b$ (n = 5) ν_{max}(KBr): 2920 (m, C—H), 1620 (s, N=C), 1610, 1510 (s, Ar), 1260, 1180 (s, C—O) cm^{-1}; δ_H(C_6D_6): 8.70 (s, 1H, N=CH),

8.63 (2H, d, J = 5 Hz, pyridine-H), 8.02 (d, J = 10 Hz, 2H, ArH), 7.25 (d, J = 5 Hz, 2H, pyridine-H), 6.85 (d, J = 10 Hz - 2H, ArH), 3.66—3.63 (m, 2H, CH_2—O), 1.71—0.99 (m, 9H, C_4H_9); m/z (%): 352.1 (M^+, 100), 351.1 (M^+ - 1, 58.2), 281.1 (HOC_6H_4-C_2N_2S-N = C-$C_5H_4N^+$, 76.4), 136.9 (30.6), 71.1 (3.0), 43.0 (31.4). Anal. $C_{19}H_{20}$-N_4OS. Calcd: C, 64.77; H, 5.68; N, 15.91. Found: C, 64.37; H, 6.03; N, 15.02.

I_c (n = 6) ν_{max}(KBr): 2930 (m, C—H), 1620 (s, N = C), 1610, 1510 (s, Ar), 1250, 1180 (s, C—O) cm^{-1}; δ_H(C_6D_6): 8.73 (s, 1H, N = CH), 8.69 (d, J = 10 Hz, 2H, pyridine-H), 8.02 (d, J = 10 Hz, 2H, ArH), 7.22 (d, J = 10 Hz, 2H, pyridine-H), 6.82 (d, J = 5 Hz, 2H, ArH), 3.61—3.58 (m, 2H, CH_2O), 1.81—0.99 (m, 11H, C_5H_{11}-aliphat); m/z (%): 366.2 (M^+, 100), 365.2 (M^+ - 1, 53.5), 281.2 (HOC_6H_4-C_2N_2S-N = C-$C_5H_4N^+$, 74.4), 137.0 (19.6), 71.2 (2.4), 43.1 (24.6). Anal. $C_{20}H_{22}$-N_5OS. Calcd: C, 65.57; H, 6.01; N, 15.30. Found: C, 64.71; H, 7.37; N, 14.54.

I_d (n = 7) ν_{max}(KBr): 2920 (m, C—H), 1620 (s, N = C), 1610, 1510 (s, Ar), 1260, 1180 (s, C—O) cm^{-1}; δ_H(C_6D_6): 8.72 (s, 1H, N = CH), 8.68 (d, J = 5 Hz, 2H, pyridine-H), 8.04 (d, J = 10 Hz, 2H, ArH), 7.23 (d, J = 10 Hz, 2H, pyridine-H), 6.84 (d, J = 5 Hz, 2H, ArH), 3.63—3.58 (m, 2H, CH_2—O), 1.80—0.95 (m, 13H, C_6H_{13}), m/z (%): 380.1 (M^+, 100), 379.1 (M^+ - 1, 59.3), 281.1 (HOC_6H_4-C_2N_2S-N = C-$C_5H_4N^+$, 76.8), 137.0 (19.23), 71.1 (2.0), 43.0 (19.4). Anal. $C_{21}H_{24}N_4OS$. Calcd: C, 66.32; H, 6.32; N, 14.74. Found: C, 65.72; H, 6.60; N, 14.18.

I_e (n = 8) ν_{max}(KBr): 2910 (m, C—H), 1620 (s, N = C), 1610, 1510 (s, Ar), 1260, 1180 (s, C—O) cm^{-1}, δ_H(C_6D_6): 8.71 (s, 1H, N = CH), 8.64 (d, J = 10 Hz, 2H, pyridine-H), 8.02 (d, J = 5 Hz, 2H, ArH), 7.25 (d, J = 5 Hz, 2H, pyridine-H), 6.83 (d, J = 5 Hz, 2H, ArH), 3.65—3.61 (m, 2H, CH_2-O), 1.88—0.89 (m, 15H, C_7H_{15}), m/z (%): 394.1 (M^+, 100), 393.0 (M^+ - 1, 49.7), 281.1 (HOC_6H_4-C_2N_2S-N = C-$C_5H_4N^+$, 71.3), 137.0 (23.2), 71.1 (4.36), 43.1 (25.95). Anal. $C_{22}H_{26}$-N_4OS. Calcd: C, 67.01; H, 6.60; N, 14.21. Found: C, 66.99; H, 7.16; N, 14.83.

I_f (n = 9) ν_{max}(KBr): 2950 (m, C—H), 1620 (s, N = C), 1610, 1510 (s, Ar), 1260, 1180 (s, C—O) cm^{-1}, δ_H(C_6D_6): 8.73 (s, 1H, N = CH), 8.69 (d, J = 10 Hz, 2H, pyridine-H), 8.02 (d, J = 10 Hz, 2H, ArH), 7.22 (d, J = 10 Hz, 2H, pyridine-H), 6.84 (d, J = 10 Hz, 2H, ArH), 3.60—3.57 (m, 2H, CH_2—O), 1.90—0.88 (m, 17H, C_8H_{17}); m/z (%): 408.0 (M^+, 100), 407.0 (M^+ - 1, 66.0), 281.0 (HOC_6H_4-C_2N_2S-N = C-$C_5H_4N^+$, 79.6), 136.9 (15.8), 71.0 (9.0), 43.0 (34.2). Anal. $C_{23}H_{28}N_4OS$. Calcd: C, 67.65; H, 6.86; N, 13.73. Found: C, 67.83; H, 7.51; N, 13.50.

I_g (n = 10) ν_{max}(KBr): 2910 (m, C—H), 1620 (s, N = C), 1610, 1510 (s, Ar), 1260, 1180 (s, C—O) cm^{-1}, δ_H(C_6D_6): 8.70 (s, 1H, N = CH), 8.67 (d, J = 10 Hz, 2H, pyridine-H), 8.02 (d, J = 10 Hz, 2H, ArH), 7.25 (d, J = 5 Hz, 2H, pyridine-H), 6.84 (d, J = 10 Hz, 2H, ArH), 3.64—3.59 (m, 2H, CH_2O), 1.90—0.87 (m, 19H, C_9H_{19}); m/z (%): 422.1 (M^+, 100), 421.1 (M^+ - 1, 59.7), 281.2 (HOC_6H_4-C_2N_2S-N = C-$C_5H_4N^+$, 83.2), 137.0 (24.8), 71.1 (3.5), 43.0 (28.8). Anal. $C_{24}H_{30}N_4OS$. Calcd.: C, 71.01; H, 8.09; N, 8.28. Found: C, 71.04; H, 8.19; N, 8.20.

Results and discussion

The transition temperatures were measured by DSC. Phase identification was made by comparing the observed textures with those in the literature.[13,14] The results were summarized in Table 1.

All of the synthesized compounds exhibit enantiotropic smectic A phase. Fig. 1(a) shows the result of differential scanning calorimetry (DSC) of compound **I_a**. On heating cycle, four peaks at 114.4, 124.9, 142.6 and 159.7℃ are observed. They are attributed to the solid-Cr_1, Cr_1-Cr_2, Cr_2-L_C phase and L_C phase-isotropic liquid phase transition, respectively. Two peaks at 146.3 and 125.2℃ on cooling cycle are transition temperatures of isotropic liquid-LC phase and LC phase-solid. The mesomorphic phase of compound **I_a** is determined by polarized optical microscopy. When heated to 142.0℃, the sample of **I_a** between glass slide and coverslip begins to melt and lots of fine grains are formed. Immediately, the fine grains coalesce and build up the polygonal textures with fan-shaped appearance. Fig. 2(a) depicts this texture of smectic A phase at a temperature of 7℃

above the solid-liquid crystal phase transition. On cooling cycle the same texture is observed.

Table 1 Transition temperature of compounds $\mathbf{I_a}$—$\mathbf{I_g}$ synthesized

Compounds	n	Transition temperatures (℃) and enthalpies (J/g)
$\mathbf{I_a}$	4	Cr 114.4 Cr_1 124.9 Cr_2 142.6 S_A 159.7 I 146.3 S_A 125.2 Recr
		(2.9) (15.2) (72.9) (11.7) (8.8) (58.3)
$\mathbf{I_b}$	5	Cr 128.0 Cr_1 134.2 S_A 163.6 I 159.4 S_A 114.8 Recr
		(44.3) (90.7) (11.7) (12.1) (77.2)
$\mathbf{I_c}$	6	Cr 129.1 S_A 170.5 I 162.2 S_A 98.2 Recr
		(87.6) (12.6) (9.1) (63.0)
$\mathbf{I_d}$	7	Cr 113.7 S 1 121.1 S_A 159.2 I 152.0 S_A 85.6 Recr
		(104.5) (36.2) (15.1) (11.3) (45.3)
$\mathbf{I_e}$	8	Cr 103.4 Cr_1 111.3 Cr_2 119.8 S_A 171.1 I 160.4 S_A 86.2 Recr
		(13.3) (39.9) (53.7) (10.7) (8.8) (53.0)
$\mathbf{I_f}$	9	Cr 118.5 S_A 162.9 I 154.5 S_A 89.0 Recr
		(60.0) (15.1) (13.6) (43.6)
$\mathbf{I_g}$	10	Cr 106.8 Cr_1 119.8 S_A 176.6 I 152.0 S_A 88.8 Recr
		(26.1) (79.8) (13.6) (11.9) (55.5)

In Fig. 1(b), DSC of compound $\mathbf{I_b}$ shows three peaks on heating cycle and two peaks on the cooling cycle. They are attributed to the solid-Cr_1, Cr_1-S_A, S_A-isotropic liquid, isotropic liquid-S_A, S_A-solid phase transition, respectively. Polygonal textures with fan-shaped appearance support the assignment of the mesomorphic phase of compound $\mathbf{I_b}$ as smectic A (Fig. 2 (b)).

The result of DSC of compound $\mathbf{I_c}$ is shown in Fig. 1(c). There are only two peaks on heating cycle. It means that when heated to the melting point the solid converts to liquid crystal phase without any crystal form transition. Two peaks on cooling cycle are attributed to isotropic liquid-S_A and S_A-solid phase transition. Fig. 2 (c) depicts the fan-shaped textures with spherulitic domains of the smectic A phase of compound $\mathbf{I_c}$ at the temperature of 4℃ below the isotropic liquid-S_A phase transition.

Compound $\mathbf{I_d}$ exhibits some different phase transition behavior from others. In Fig. 1(d), three peaks at 113.7, 121.1 and 159.2℃ are clearly observed on heating cycle. These three peaks are attributed to the solid-S_1, S_1-S_A and S_A-isotropic liquid phase transition, respectively. During the cooling cycle S_1 phase does not reproduce because there are only two peaks on cooling cycle curve. By means of polarizing microscopy the transition temperature range between 113.7 and 121.1℃ is attributed to a smectic phase range (S_1). This range is so small (8℃) that no texture photos can be taken for it neither this liquid crystalline phase can be exactly characterized. Furthermore, during the cooling cycle only the texture of smectic A phase is observed and S_1 phase does not reproduce. Fig. 2(d) shows the texture of smectic A phase of compound $\mathbf{I_d}$.

The result of DSC of compound $\mathbf{I_e}$ is similar to that of compound $\mathbf{I_a}$, four peaks on heating cycle and two peaks on cooling cycle. The DSC data of compound $\mathbf{I_f}$ is similar with those of compound $\mathbf{I_c}$, with two peaks on heating and cooling cycle, respectively. And the result of DSC of compound $\mathbf{I_g}$ shows three peaks on heating cycle and two peaks on cooling cycle. Fig. 2 (e)—(g) depict the polygonal textures and fan-shaped textures of the smectic A phase of $\mathbf{I_e}$—$\mathbf{I_g}$.

It is interesting that these compounds reported here exhibit a different phase transition behavior on heating cycle. $\mathbf{I_a}$ and $\mathbf{I_e}$ exhibit two crystalline phases and smectic A phase. $\mathbf{I_b}$ and $\mathbf{I_g}$ show one crystalline phase and smectic A phase. $\mathbf{I_c}$ and $\mathbf{I_f}$ only show smectic A phase. And only $\mathbf{I_d}$ exhibits S_1 phase and S_A phase. But on cooling cycle the phase transition behavior of all compounds is quite similar, and they all exhibit only a smectic A phase and no other phase is observed. The relation between the phase transition behavior and the carbon chain length of the alkoxyl is not clear at this moment. Further study is underway.

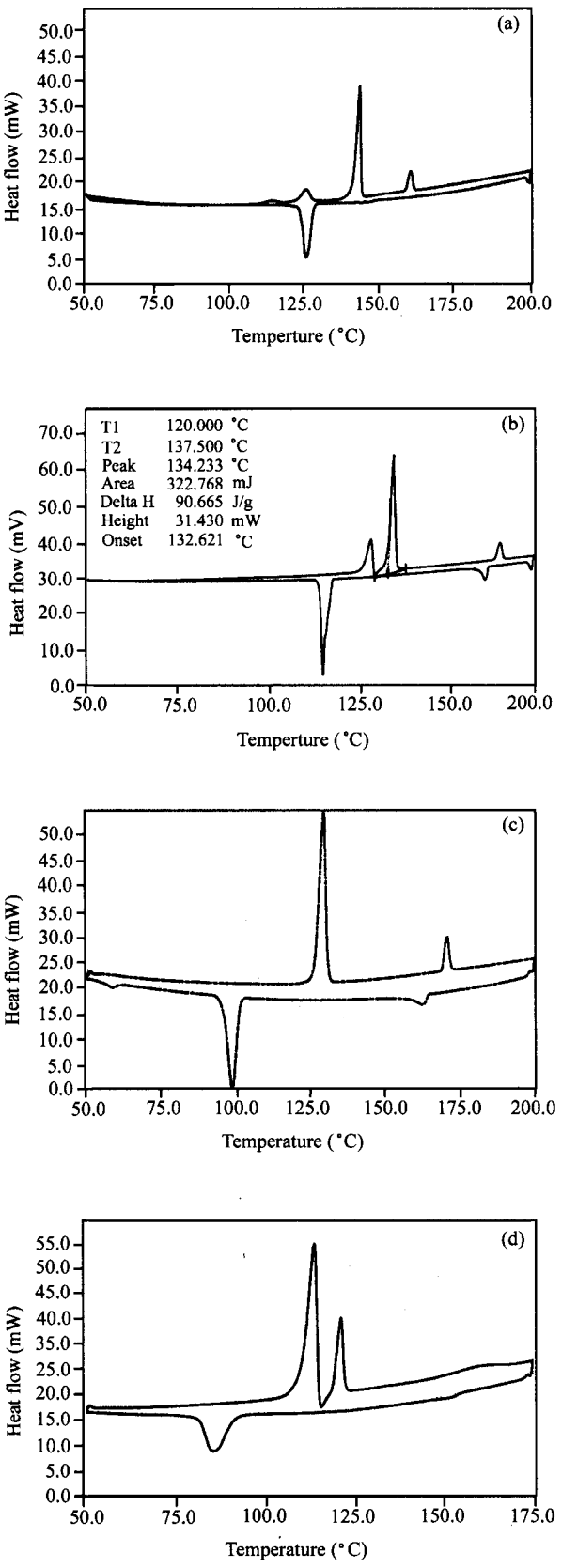

(a) (149℃, on heating)

(b) (147℃, on cooling)

(c) (158℃, on cooling)

(d) (150℃, on cooling)

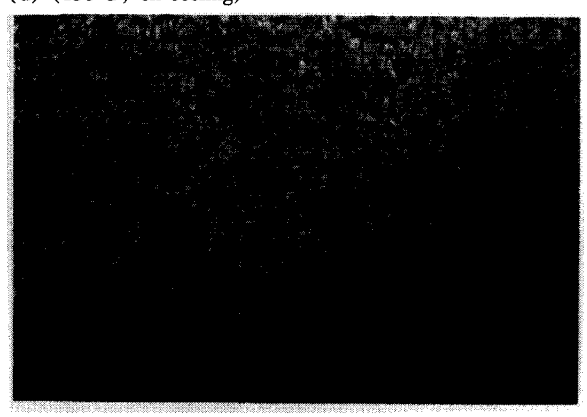

Fig. 1 DSC of compounds $\mathbf{I_a}$—$\mathbf{I_d}$.

(e) (131℃, on cooling)

(f) (130℃, on cooling)

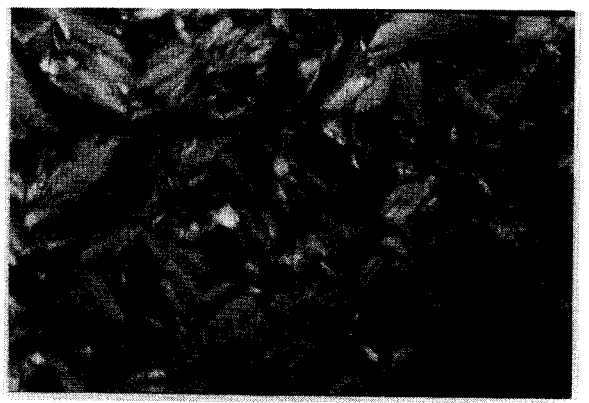

(g) (149℃, on cooling)

Fig. 2 Texture of compounds $\mathbf{I_a}$—$\mathbf{I_g}$.

It is further noted that an increase in the clearing point occurs with elongating length of the alkoxyl chain (Fig. 3). The usual odd-even effect can also be found in the mesophase-isotropic liquid transitions (Fig. 3).[15]

These compounds can be compared with the similar Schiff's bases without 1, 3, 4-thiadiazole ring. 4-*n*-Alkoxy-*N*-(4-pyridylmethylene) anilines[10] (Scheme 3) are not mesomorphic. By introducing a 1,3,4-thiadiazole ring into the molecule, the polarizability and rigidity of the molecule are enhanced and stable mesomorphases are produced.

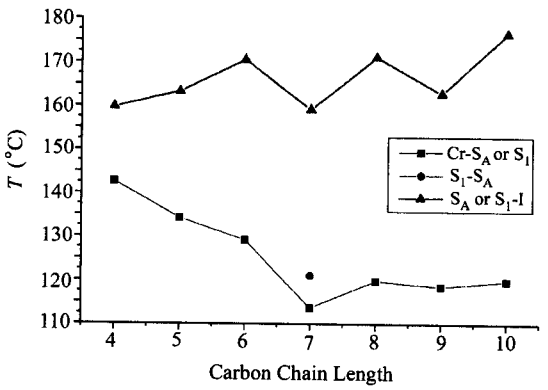

Fig. 3 The variations of mesogen phase temperature with carbon chain length.

Scheme 3

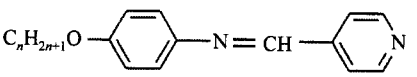

Because the substituents occupy the 2,5-position of the 1,3,4-thiadiazole ring, the molecule exhibits a herringbone structure. And a herringbone structure is probably related with a dimeric liquid crystalline structure.[16] It can be supposed that the compounds synthesized may have bilayer structures like those molecules associated with nitro (NO_2) and cyano (CN) as terminal groups.[14] Further investigations of the molecular arrangement are still in progress.

References

1 Zaschke, H.; Wiss, Z. *Math. Naturwiss.* **1980**, *R29*, 35.

2 Deutscher, H. J.; Vorbradt, H. M.; Zaschke, H. *Z. Chem.* **1981**, *21*, 9.

3 Bartulín, J.; Zúñiga, C.; Ramírez, A.; Muller, H.; Taylor, T. R. *Mol. Cryst. Liq. Cryst.* **1990**, *185*, 131.

4 Demus, D.; Zaschke, H. *Flüssige Kristalle in Tabellen*, VEB Deutscher Verlag für Grundstoffindustrie, Leipzig, **1984**.

5 Dimitrowa, K.; Hauschild, J.; Zaschke, H.; Schubert,

H. *J. Prakt. Chem.* **1980**, *322*, 933.
6 Schäfer, W.; Rosenfeld, U.; Zaschke, H.; Stettin, H.; Kresse, H. *J. Prakt. Chem.* **1989**, *331*, 631.
7 Parra, M.; Belmar, J.; Zunza, H.; Zúñiga, C.; Villouta, S.; Martínez, R. *Bol. Soc. Chill. Quím.* **1993**, *38*, 325.
8 Parra, M.; Belmar, J.; Villouta, S.; Martínez, R. *Bol. Soc. Chill. Quím.* **1995**, *40*, 175.
9 Paleos, C. M.; Tsiourvas, D. *Angew. Chem. Int. Ed. Engl.* **1995**, *34*, 1696.
10 Marcos, M.; Ros, M. B.; Serrano, J. L. *Chem. Mater.* **1990**, *2*, 748.
11 Castellano, J. A.; Chan, S. O.; Mccaffrey, M. T. *Mol. Cryst. Liq. Cryst.* **1973**, *27*, 417.
12 Yan, X.; Wanfang, L.; Zihou, T. *Mol. Cryst. Liq. Cryst.* in press.
13 Demus, D.; Richter, L. *Textures of Liquid Crystals*, Verlag Chemie, Weinheim, **1987**.
14 Gray, G. W.; Goodby, J. W. *Smectic Liquid Crystals, Textures and Structures*, Heyden and son, Philddephia, **1984**.
15 Demus, D. *Z. Chem.* **1975**, *15*, 1.
16 Aoki, Y.; Nohira, H. *Ferroelectrics* **1996**, *178*, 213.

(E200011239 JIANG, X. H.; LING, J.)